Immunity
Article

The DNA Sugar Backbone 2′ Deoxyribose Determines Toll-like Receptor 9 Activation

Tobias Haas,[1] Jochen Metzger,[2] Frank Schmitz,[1] Antje Heit,[1] Thomas Müller,[1] Eicke Latz,[3] and Hermann Wagner[1,*]
[1]Institut für Medizinische Mikrobiologie, Immunologie und Hygiene, Technische Universität München, Trogerstrasse 30, 81675 München, Germany
[2]Institut für Klinische Chemie und Pathobiochemie, Klinikum rechts der Isar, Technische Universität München, Ismaningerstrasse 22, 81675 München, Germany
[3]University of Massachusetts Medical School, Division of Infectious Diseases and Immunology, 364 Plantation Street, Worcester, MA 01605, USA
*Correspondence: h.wagner@lrz.tum.de
DOI 10.1016/j.immuni.2008.01.013

SUMMARY

CpG motifs within phosphorothioate (PS)-modified DNA drive Toll-like receptor 9 (TLR9) activation, but the rules governing recognition of natural phosphodiester (PD) DNA are less understood. Here, we showed that the sugar backbone determined DNA recognition by TLR9. Homopolymeric, base-free PD 2′ deoxyribose acted as a basal TLR9 agonist as it bound to and activated TLR9. This effect was enhanced by DNA bases, even short of CpG motifs. In contrast, PS-modified 2′ deoxyribose homopolymers acted as TLR9 and TLR7 antagonists. They displayed high affinity to both TLRs and did not activate on their own, but they competitively inhibited ligand-TLR interaction and activation. Although addition of random DNA bases to the PS 2′ deoxyribose backbone did not alter these effects, CpG motifs transformed TLR9-inhibitory to robust TLR9-stimulatory activity. Our results identified the PD 2′ deoxyribose backbone as an important determinant of TLR9 activation by natural DNA, restrict CpG-motif dependency of TLR9 activation to synthetic PS-modified ligands, and define PS-modified 2′ deoxyribose as a prime effector of TLR9 and TLR7 inhibition.

INTRODUCTION

Toll-like receptors (TLRs) are a family of nonclonal pattern-recognition receptors that recognize conserved pathogen-associated molecular patterns (PAMPs). Under homeostatic conditions, TLRs discriminate "non-self" from "self" in that they do not sense host-derived "self-molecules" but become activated by PAMPs during infection (Akira et al., 2006; Janeway and Medzhitov, 2002). In mammals, distinct TLRs recognize PAMPs present on nucleic acids, carbohydrates, lipids, and proteins (Akira et al., 2006; Beutler et al., 2006). Although the majority of TLRs (TLR1, TLR2, TLR4, TLR5, TLR6, and TLR11) are expressed at the cell surface, the TLRs that recognize nucleic acids, i.e., TLR3 (sensing double-stranded RNA [dsRNA] [Alexopoulou et al., 2001]), TLR7 and TLR8 (sensing single-stranded RNA [ssRNA] [Diebold et al., 2004; Heil et al., 2004]), and TLR9 (sensing single-stranded CpG-DNA [Hemmi et al., 2000]), are confined to intracellular compartments in which they reside in endosomes (Akira et al., 2006; Beutler et al., 2006). Ligand binding by TLR3, TLR7, TLR8, and TLR9 occurs in the acidic environment of the endosome (Hacker et al., 1998; Leifer et al., 2004) and causes cellular activation presumably by stabilizing preformed TLR dimers or inducing TLR-dimer formation (Kindrachuk et al., 2007; Latz et al., 2007; Weber et al., 2003).

Species specificity of and sequence requirements for the activation of TLR9 by ssDNA (Bauer et al., 2001; Krieg, 2002) have primarily been elucidated with synthetic oligodeoxynucleotides (ODNs) with a phosphorothioate (PS)-modified backbone (see Figure S1A available online) to improve nuclease resistance (Krieg, 2002) and cellular uptake (Sester et al., 2000). Optimal CpG motifs for murine TLR9 activation were thus defined as a nonmethylated CpG dinucleotide flanked by two 5′ purines and two 3′ pyrimidines. Given that cytosine methylation or inversion of CpG dinucleotides to GpC predominantly abolishes the ability of PS ODNs to activate TLR9 (Krieg, 2002), the paradigm has evolved that discrimination of "self-DNA" versus pathogen-derived "non-self-DNA" relies on such CpG motifs (PAMPs), which are abundant in pathogen-derived DNA but scarce in mammalian "self-DNA" (Bird, 1986). Ligand-binding studies, however, have yielded contradictory results with respect to the ability of TLR9 to selectively bind ssDNA in a sequence-specific manner (Latz et al., 2004; Yasuda et al., 2006). Furthermore, B cells and dendritic cells (DCs) sense "self-DNA" via TLR9 upon anti-DNA autoantibody-mediated DNA entry into the endolysosomal compartment (Boule et al., 2004; Leadbetter et al., 2002). In addition, enforced endosomal translocation of vertebrate DNA in complex with the antimicrobial peptide LL37 or with the cationic lipid N-[1-(2,3-dioleoyloxy)]-N,N,N-trimethylammonium propan methylsulfate (DOTAP) induces TLR9 activation (Lande et al., 2007; Yasuda et al., 2006; Yasuda et al., 2005). Altogether, these findings suggest that the endosomal localization of TLR9 prevents constant activation by "self-DNA" under homeostatic conditions. Along these lines, there is evidence that a hybrid TLR composed of the extracellular domain of TLR9 (TLR9-ect) and the cytoplasmic and transmembrane domains of TLR4, which was reported to localize to the cell surface, recognizes mammalian DNA (Barton et al., 2006), even though these findings are controversial (Leifer et al., 2006). We therefore envisioned two possible scenarios for the activation of TLR9 by "self-DNA": Either CpG motifs in mammalian DNA

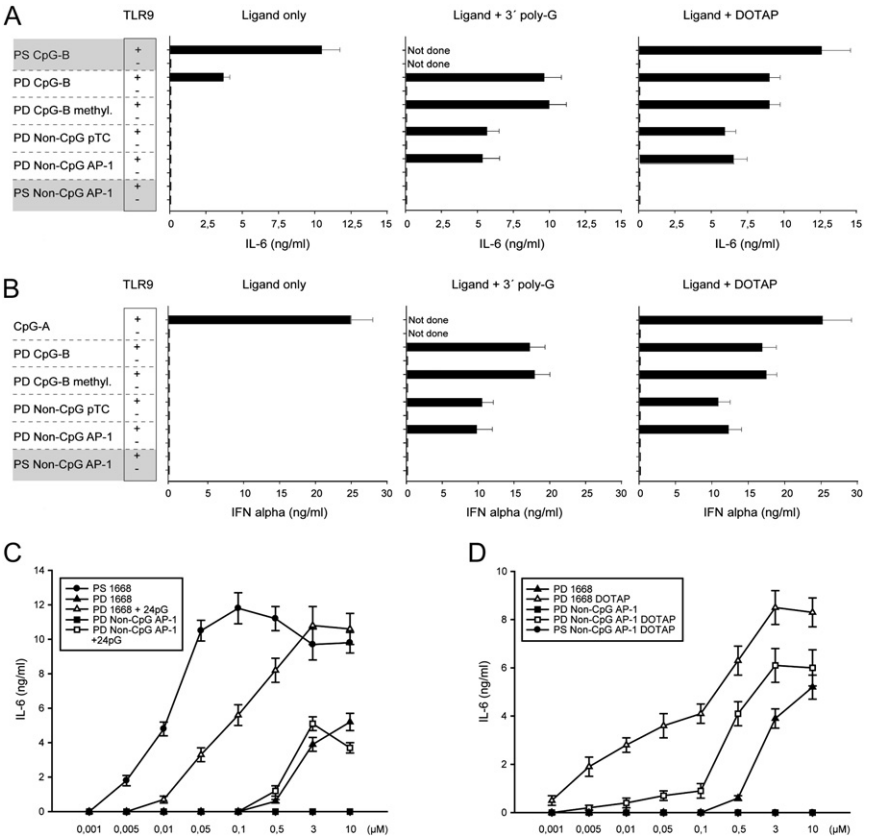

Figure 1. CpG-Independent TLR9 Activation by Natural PD ODNs

(A and B) WT or *Tlr9*$^{-/-}$ Flt3L-DCs (1 × 10^6/well) were incubated for 18 hr with 3 μM ODNs, ODNs 3′ extended with 24Gs, or ODNs complexed to DOTAP. IL-6 (A) and IFN-α (B) concentrations were detected in culture supernatants by enzyme-linked immunosorbant assay.

(C and D) WT Flt3L-DCs (1 × 10^6/well) were incubated for 18 hr with indicated concentrations of ODNs alone or ODNs 3′ extended with 24Gs (C) and ODNs alone or ODNs complexed to DOTAP (D). IL-6 concentrations were detected in culture supernatants by enzyme-linked immunosorbant assay. Values for PD 1668 and PD non-CpG AP-1 in (C) and (D) are taken from the same set of experiments. Mean values and standard deviations of three independent experiments are shown in (A)–(D).

are scarce yet sufficient for activation, or natural DNA with a phosphodiester (PD) backbone has an inherent, sequence-independent stimulatory capacity, a quality that may have been obscured in experiments using PS-modified DNA. Consequently, we asked whether different rules apply for TLR9 activation by natural PD versus PS-modified DNA. Here, we describe that the DNA sugar backbone 2′ deoxyribose represents a prime determinant for ssDNA-TLR9 interactions. In its natural PD version, base-free 2′ deoxyribose homopolymers act as basal TLR9 agonists, and DNA bases, even short of CpG motifs, enhance agonist activity. In their PS-modified version, however, 2′ deoxyribose homopolymers act as TLR9 and TLR7 antagonists. Random bases do not alter antagonist function, but DNA sequences containing CpG motifs transform TLR9-inhibitory to robust TLR9-stimulatory activity.

Thus, we have shown that TLR9 senses natural, unmodified ssDNA present in the endosome in a CpG-independent manner, on the basis of the inherent stimulatory potential of the PD 2′ deoxyribose backbone. The DNA sequence can modulate the strength of the response, but strict CpG-motif dependency of TLR9 activation is an exclusive characteristic of PS-modified ssDNA, which otherwise is a TLR9 and TLR7 antagonist.

RESULTS

3′ Poly-G Extension Reveals TLR9 Agonist Activity of PD Non-CpG DNA

On the basis of reports that, similar to cationic lipids, 3′ extension of PD ODNs with polyguanosine (poly-G) tails not only protects against DNase degradation (Bishop et al., 1996) but also drives enhanced endosomal translocation (Dalpke et al., 2002), we first tested whether the poor TLR9 activation by single-stranded PD CpG ODNs can be improved by 3′ PD poly-G extension. CpG ODNs are commonly classified into A or B type according to their potential to preferentially induce TLR9-dependent interferon-α (IFN-α) production or proinflammatory cytokine production and DC maturation, respectively (Verthelyi et al., 2001; Krieg, 2002). We observed enhanced cellular uptake (Figure S2A) and cytokine production (Figure S2B) by Flt3L-DCs (containing a mixture of plasmacytoid [p] DCs and myeloid [m] DCs) upon 3′ PD poly-G extension of B type PD CpG ODN 1668 (CpG-B), depending on the length of the poly-G tail (for sequences and chemical structures, see Figure S1). Of note, 3′ PD poly-G extension (24 Gs) not only improved the poor TLR9-stimulatory potential of DNase-sensitive PD CpG-B but also reconstituted it, at high concentrations, to values similar to canonical PS CpG-B (Figure S2B; see Figure 1C for titration). It also conveyed TLR9-dependent IFN-α-inducing activity (Figure S2C), to date considered a sequence-specific hallmark of A type CpG (CpG-A) (Kerkmann et al., 2005; Verthelyi et al., 2001).

We speculated that enhanced endosomal translocation through 3′ PD poly-G extension may also lead to TLR9 activation by PD ODNs devoid of canonical unmethylated CpG-motifs (PD non-CpG ODNs). Indeed, upon 3′ PD poly-G extension (24 Gs), both methylated PD CpG-B and PD ODNs lacking canonical CpG motifs (e.g., PD non-CpG ODN AP-1 and PD non-CpG ODN pTC; Figure S1B) triggered TLR9-dependent IL-6 and IFN-α production (Figures 1A and 1B) as well as upregulation of CD86 costimulatory molecules (Figure S2D) by Flt3L-DCs. Across a wide range of ODN concentrations, the TLR9-activating potential of 3′ poly-G extended PD ODNs was similar to that of PD ODNs complexed to N-[1-(2,3-dioleoyloxy)]-N,N,N-trimethylammonium propan methylsulfate (DOTAP) (Figures 1C and 1D; Figure S2E). These results imply that the previously reported TLR9-stimulatory potential of PD non-CpG single-stranded

ODNs complexed to DOTAP (Yasuda et al., 2006) is not merely a transfection-agent-related phenomenon but rather reflects the ability of TLR9 to recognize and react to unmodified PD ODNs short of canonical CpG-motifs. In contrast, PS-modified ODNs lacking CpG-motifs did not activate TLR9, even when complexed to DOTAP or 3′ extended by poly-Gs (Figures 1A, 1B, and 1D; Figure S2E).

To exclude the possibility that the data on TLR9 activation by endosomally translocated PD non-CpG ODN AP-1 may have been biased by the CG dinucleotide present in the AP-1 sequence (Although it does not qualify as a canonical CpG motif, noncomplexed PS or PD non-CpG ODN AP-1 is therefore TLR9 "inactive."), we repeated this set of experiments with non-CpG ODN AP-1 molecules that had the CG dinucleotide eliminated by substituting A for C. No relevant differences in the TLR9-stimulatory potential were seen when compared to the original non-CpG ODN AP-1 sequence (data not shown).

Poly-G-extended PD ODN sequences efficiently form G-tetrads and are preferentially retained in early endosomes (data not shown). We have shown that both 3′ PD poly-G-extended or DOTAP-complexed PD CpG ODN and PD non-CpG ODN induce IFN-α production (Figure 1B and Figure S2E), the latter with lower efficiency. Our data thus support the notion that PD ODN multimerization is sufficient for sequence-independent IFN-α induction (Guiducci et al., 2006; Honda et al., 2005) at optimal ligand concentrations because it leads to enhanced cellular uptake and early endosomal retention and thus to ligand-induced activation of the TLR9-MyD88-IRF-7 signaling pathway. Indeed, IFN-α production was completely abolished in TLR9- (Figure 1B), MyD88- (not shown), and IRF-7-deficient cells (Figure S3A). When pDCs and mDCs were sorted from mixed Flt-3L DC cultures, IFN-α was found to be exclusively produced by pDCs, whereas the main source of proinflammatory cytokines such as IL-6 were mDCs (Figure S3B). Overall, IFN-α induction by multimerized PD ODNs relied on mechanisms similar to those previously defined for canonical CpG-A.

The PD Sugar Backbone Licenses DNA for TLR9 Activation

Certain PS modified non-CpG ODN sequences, including those containing a GGGG motif (immunoregulatory sequences [IRSs]), have been described to inhibit ligand-driven TLR9 and/or TLR7 activation in a sequence-dependent manner (Barrat et al., 2005; Duramad et al., 2005; Gursel et al., 2003). When we used the TLR9-relevant IRS ODN sequences 869 and 954 (Barrat et al., 2005) with a natural PD sugar backbone and complexed them to DOTAP, they actually activated DCs to produce IL-6 (Figure 2A) and IFN-α in a TLR9-dependent manner (data not shown). Because changing the IRS backbone from PS to PD converted TLR9 inhibition into TLR9 stimulation, the importance of the DNA sugar backbone for the interaction between DNA and TLR9 became apparent. This conclusion was supported by the observation that the TLR9-stimulatory activity of PD non-CpG ODN AP-1 complexed to DOTAP was abolished in a hybrid PD AP-1 in which the DNA-backbone sugar 2′ deoxyribose was replaced by the RNA sugar ribose (ribose-AP-1; Figure 2B and Figure S4A). Similar results were obtained when PD poly-G-extended PD ODN AP-1 was compared to PD poly-G-extended PD ribose-AP-1 (data not shown). In terms of TLR9 activation,

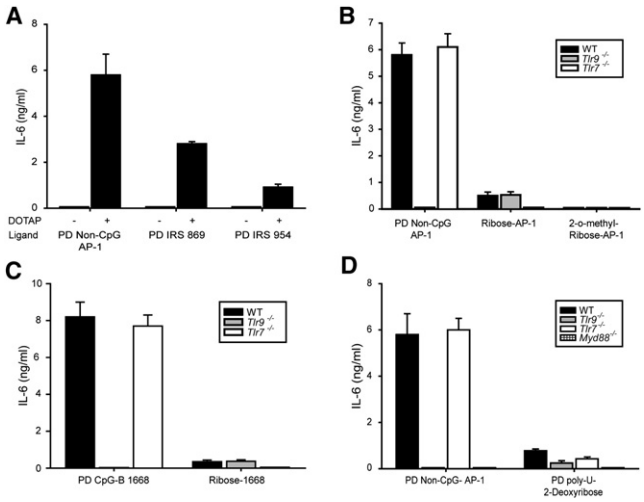

Figure 2. Role of the Sugar Backbone in TLR9 and TLR7 Activation

(A) WT Flt3L-DCs (1×10^6/well) were incubated for 18 hr with 3 μM of PD ODNs alone or PD ODNs complexed to DOTAP. IL-6 concentrations were detected in culture supernatants by enzyme-linked immunosorbant assay.

(B and C) WT, *Tlr9*$^{-/-}$ or *Tlr7*$^{-/-}$ Flt3L-DCs (1×10^6/well) were incubated for 18 hr with 3 μM of indicated PD ODN or hybrid DNA/RNA molecules complexed to DOTAP. IL-6 concentrations were detected in culture supernatants by enzyme-linked immunosorbant assay.

(D) WT, *Tlr9*$^{-/-}$, *Tlr7*$^{-/-}$, or *Myd88*$^{-/-}$ Flt3L-DCs (1×10^6/well) were incubated for 18 hr with 3 μM of PD ODNs or PD poly-U-2′ deoxyribose complexed to DOTAP. IL-6 concentrations were detected in culture supernatants by enzyme-linked immunosorbant assay. Mean values and standard deviations of three independent experiments are shown in (A)–(D).

dominance of the sugar backbone over the nucleic-acid base component of ODNs was also observed with a hybrid containing a canonical CpG motif, ribose 1668 (Figure 2C and Figure S4B). Thus, otherwise stimulatory ssDNA is not recognized by TLR9 when the DNA-backbone sugar 2′ deoxyribose is replaced with the RNA-backbone sugar ribose, irrespective of its base sequence. However, both ribose AP-1 and ribose 1668 triggered minimal but marked TLR7 activation, whereas 2-o-methyl-modified ribose AP-1 did not (Figures 2B and 2C; Figures S4A and S4B), indicating a ribose-backbone-instructed, sequence-independent activation mode of TLR7. In context, when the DNA-backbone sugar PD 2′ deoxyribose was present, it rendered TLR9 permissive even for nucleic-acid bases usually not present in natural DNA, because a hybrid 20-mer combining a PD 2′ deoxyribose backbone with aligned uracil bases (poly-U-2′ deoxyribose; see Figure S1A) activated both TLR9 and TLR7. *Tlr7*$^{-/-}$ or *Tlr9*$^{-/-}$ cells both showed activation, whereas *Myd88*$^{-/-}$ and *Tlr7*$^{-/-}$ *Tlr9*$^{-/-}$ cells were each unresponsive (Figure 2D; Figure S4C and data not shown). These data show that TLR9 strictly requires 2′ deoxyribose, which licenses ODNs for activation even in the absence of typical DNA bases. In contrast, TLR7 is more liberal with respect to backbone restrictions, because both ribose and 2′ deoxyribose backbones were accepted for activation.

PD 2′ Deoxyribose Homopolymers Act as TLR9 Agonists

The findings described above suggested a dominant role of PD 2′ deoxyribose in TLR9-mediated DNA recognition. We therefore

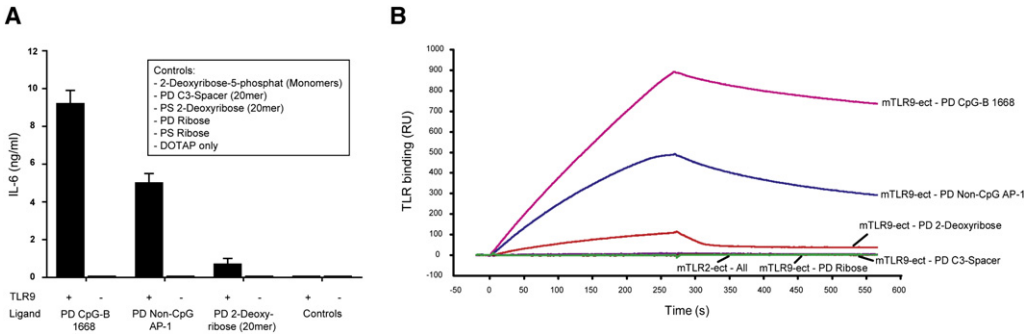

Figure 3. PD 2′ Deoxyribose Homopolymer Is a TLR9 Agonist

(A) WT or *Tlr9*$^{-/-}$ Flt3L-DCs (1 × 10^6/well) were incubated for 18 hr with 3 μM of indicated ODN (20-mer), PD 2′ deoxyribose (20-mer), or controls, all complexed to DOTAP. IL-6 concentrations were detected in culture supernatants by enzyme-linked immunosorbant assay. Mean values and standard deviations of at least three independent experiments are shown.

(B) SPR analysis of 100 nM mTLR9-ect binding to biotinylated ODN or sugar-backbone molecules immobilized at equimolar amounts on a streptavidin-coated biosensor chip. mTLR2-ect was used as a control. No mTLR2-ect binding to any of the ODNs or sugar-backbone molecules was detected.

analyzed whether PD 2′ deoxyribose (20-mer, base free) itself activated TLR9. Although 3′ poly-G-extended PD 2′ deoxyribose homopolymers failed to activate TLR9 (not shown), PD 2′ deoxyribose homopolymers complexed to DOTAP caused low but substantial TLR9-dependent cell activation (Figure 3A and Figure S4D). No stimulatory activity was observed with 2′ deoxyribose-5-phosphate monomers, PD C3 spacer (20-mer; 2′ deoxyribose replaced by three linear C atoms, conserving the distance between linking phosphodiester groups; see Figure S1A), PS-modified 2′ deoxyribose (20-mer), or PD or PS ribose (20-mer); each complexed to DOTAP (Figure 3A). These data suggested that base-free PD 2′ deoxyribose homopolymers act as agonists for TLR9.

To strengthen our confidence in the ability of the base-free PD DNA sugar backbone to activate TLR9, we determined whether PD 2′ deoxyribose (20-mer) directly binds to TLR9. Surface plasmon resonance (SPR) analysis at acidic pH revealed robust binding of PD CpG-B ODN 1668 and intermediate binding of PD non-CpG ODN AP-1 to the ectodomain of murine TLR9 (mTLR9-ect) but not to that of TLR2 (mTLR2-ect) (Figure 3B), whereas base-free PD 2′ deoxyribose homopolymers displayed low, but marked, specific binding to mTLR9-ect; PD C3 spacer and PD ribose homopolymers were both negative. These data corroborated the finding that PD 2′ deoxyribose homopolymers act as TLR9 agonists and also explained why the ribose substitution within an ODN sugar backbone abrogated TLR9 activity (Figures 2B and 2C; Figures S4A and S4B).

PS-Modified 2′ Deoxyribose Homopolymers Bind to TLR9 and TLR7 with High Affinity

In order to evaluate the role of the PS modification in DNA-TLR9 interactions, we resorted to a luminescent-proximity assay (AlphaScreen) based on the transfer of singlet oxygen between closely opposed donor and acceptor molecules (Latz et al., 2007). In this system, we again observed marked, dose-dependent, and specific binding of stimulatory PD 2′ deoxyribose homopolymers yet enhanced binding of PD non-CpG ODN AP-1 and of PD CpG-B ODN 1668 to the ectodomain of TLR9 (human; hTLR9-ect). PD C3 spacer and both PD and PS ribose homopolymers did not bind to hTLR9. Interestingly, the affinity of nonstimulatory base-free PS 2′ deoxyribose homopolymers to hTLR9 was approximately two orders of magnitude higher than that of PD 2′ deoxyribose homopolymers (Figure 4A). Of note, both PD and PS 2′ deoxyribose homopolymers also bound to hTLR7-ect with affinities similar to those defined for hTLR9-ect, in that PD 2′ deoxyribose showed low but marked hTLR7-ect affinity and PS 2′ deoxyribose showed high hTLR7-ect affinity (Figure 4B). In addition, PD ODNs (PD CpG-B ODN 1668 and PD non-CpG ODN AP-1) showed intermediate hTLR7-ect affinity, also comparable to their affinity to hTLR9-ect (data not shown). PD and PS ribose, in contrast, displayed specific, low-affine binding only to hTLR7-ect but not to hTLR9-ect (Figure 4C). The finding that the DNA-backbone sugar PD 2′ deoxyribose binds both to TLR9 and TLR7 complements our functional data on TLR7 activation by PD poly-uracil 2′ deoxyribose (Figure 2D). Furthermore, the selective affinity of TLR7 (but not of TLR9) to the RNA sugar backbone ribose (PD or PS) allows for a ribose-backbone-instructed activation of TLR7 as seen with thymidine, but not uracil, containing ribose AP-1 and ribose 1668 hybrids (Figures 2B and 2C). Finally, both TLR7 and TLR9 appear permissive for atypical bases (thymidine and uracil, respectively), yet only TLR7 is liberal with respect to the nucleotide backbone, in that TLR7 accepts both PD ribose and PD 2′ deoxyribose backbones for binding and activation.

PS-Modified 2′ Deoxyribose Homopolymers Act as TLR9 and TLR7 Antagonists

The observation that nonactivating PS 2′ deoxyribose homopolymers display high affinity to both TLR9 and TLR7 suggested that they might function as competitive inhibitors of TLR9 and TLR7 activation. In support, plasmon-resonance analysis revealed dose-dependent inhibition of PD CpG-B ODN binding to mTLR9-ect by PS 2′ deoxyribose (20-mer) (Figure 5A). PS 2′ deoxyribose linking random bases (e.g., PS non-CpG ODN AP-1; Figure S5A) and PS IRS ODN 869 (Figure S5B) displayed similar inhibition. In contrast, PD 2′ deoxyribose homopolymers exhibited low competitive effects only at very high concentrations, consistent with their comparatively low affinity to TLR9 (Figure 5B). On a functional level, base-free PS 2′ deoxyribose homopolymers dose-dependently inhibited PD CpG-B-induced

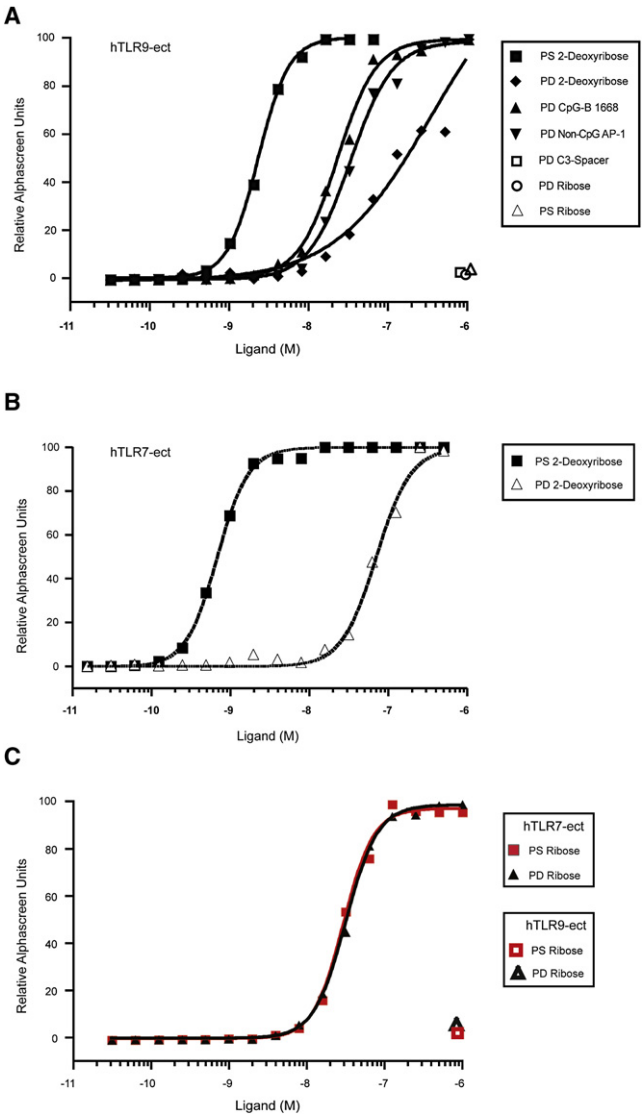

Figure 4. PS 2′ Deoxyribose Homopolymer Displays High Affinity to TLR9 and TLR7

(A–C) AlphaScreen (homogenous ligand-binding assay) assessment of hTLR9-ect (A and C) and hTLR7-ect (B and C) binding to biotinylated ODNs or sugar-backbone molecules. hTLR2-ect was used as a control. No hTLR2-ect binding to any of the ODNs or sugar-backbone molecules was detected.

TLR9-mediated cytokine responses in vitro (Figures 6A and 6B) and in vivo (Figure 6C). Again, PS IRS ODN 869 or 954 (Figure 6B) or random-base PS non-CpG ODN AP-1 (Figure S5C) manifested comparable inhibition. Interestingly, the DNA sugar backbone PS 2′ deoxyribose also inhibited PD RNA (20-mer; oligoribonucleotide [ORN] AP-1)-mediated (Figure 6D) or R848-mediated TLR7 activation in DCs, as did PS non-CpG ODN AP-1 or even PS CpG-B ODN (data not shown), similar to TLR7-inhibitory PS IRS ODN 661 (Barrat et al., 2005). Of note, inhibition of ligand-induced TLR9 and TLR7 activation by PS-modified 2′ deoxyribose homopolymers or PS ODN was TLR specific because TLR3 activation by poly I:C, TLR2 activation by Pam3Cys, and TLR4 activation by LPS were all unaffected (data not shown).

With allowance for sequence-specific modulatory effects (Barrat et al., 2005), these data imply that the PS-modified 2′ deoxyribose backbone represents the dominant determinant of competitive TLR9 and TLR7 inhibition by inhibitory PS ODNs. Importantly, though, the TLR9-inhibitory quality of PS ODNs is overcome in the presence of a canonical CpG motif because PS CpG ODN successfully convert the high TLR9 affinity of a PS-modified molecule into robust TLR9-activation (Figures 1A and 1C; Figure S2B).

DISCUSSION

Our results uncover a previously unappreciated role of the DNA sugar backbone 2′ deoxyribose in ssDNA recognition by TLR9. In its natural PD form, the base-free 2′ deoxyribose backbone binds to TLR9 with low affinity and provides basal activation upon enforced translocation into TLR9-positive endosomes. Any DNA bases, and in particular CpG motifs, linked via the PD sugar backbone, increases both TLR9 affinity and activation. In quantitative terms, base-free PD 2′ deoxyribose homopolymers displayed ~10% and PD non-CpG ODN displayed ~60% of the TLR9 activation potential of PD CpG-B ODNs, as read out by IL-6.

These characteristics of PD ODNs differ from PS-modified ODNs. PS-modified 2′ deoxyribose homopolymers bind to TLR9 and surprisingly also to TLR7 ~100-fold more strongly than PD 2′ deoxyribose homopolymers, lack stimulatory activity, but competitively inhibit ligand-induced TLR9 and TLR7 stimulation. Although random DNA bases do not affect the antagonist activity of PS 2′ deoxyribose, CpG motifs reverse this dominant-negative effect on TLR9, translating high PS ODN TLR9 affinity into strong TLR9 stimulation. Our data do not provide an answer as to how this CpG-dependent effect is brought about on a mechanistic level; we believe that the crystal structure of TLR9, once available, may provide a solution. The stimulatory power of PS CpG-B ODNs turns out to be ~10-fold greater than that of PD CpG-B ODNs, most likely due to high TLR9 affinity together with high stability against endosomal DNases. As a consequence, even very low extracellular concentrations of PS CpG-B ODNs lead to robust stimulation of endosomal TLR9. Overall, these data imply that both the strict CpG-motif dependency as well as the remarkably high TLR9 affinity are exclusive characteristics of PS-modified ODNs, which represent promising immunopharmacons (PS CpG-B [Krieg, 2002], PS IRS [Barrat et al., 2005], etc.) but do not faithfully mimic the interaction of natural PD ODNs with TLR9.

Given that TLRs that recognize nucleic acids (TLR3, TLR7, TLR8, and TLR9) are located in endosomes (Akira et al., 2006; Beutler et al., 2006), it is likely that both the endosomal concentration as well as the respective TLR9 affinity of DNA ligands will influence the TLR9 response. Because uptake of natural PD ODN by immune cells is poor (Krieg, 2002; Sester et al., 2000), we used G-tetrad-mediated multimerization of single-stranded PD ODN by 3′ poly-G extension or complex formation with DOTAP to increase DNase resistance and enhance cellular uptake. Upon multimerization or complex formation, we observed robust endosomal translocation of PD 2′ deoxyribose

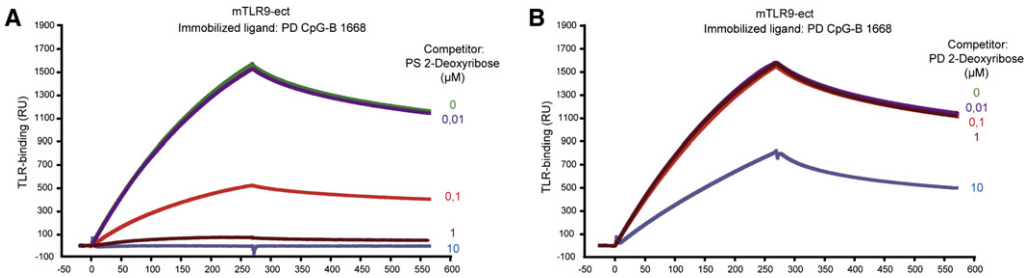

Figure 5. PS 2′ Deoxyribose Homopolymer Is a Competitive Inhibitor of TLR9 Ligand Binding

(A and B) SPR analysis of 200 nM mTLR9-ect binding to biotinylated PD CpG-B 1668 immobilized on a streptavidin-coated biosensor chip in the presence or absence of different concentrations of competing PS (A) or PD (B) 2′ deoxyribose (20-mer).

homopolymers and PD ODNs similar in magnitude to that of PS ODN. This allowed us to compare the TLR9 immunobiology of natural PD versus modified-PS ODNs under almost normalized endosomal concentrations. These conditions revealed the TLR9-stimulatory potential of base-free PD 2′ deoxyribose homopolymers and of natural PD non-CpG ODNs in plasmacytoid (p) DC- and myeloid (m) DC-containing Flt3L-cultured bone-marrow cells. TLR9 activation in mDCs occurs in late endosomes and causes production of proinflammatory cytokines, whereas IFN-α induction in pDCs depends on retention of multimerized ODN ligands in TLR9-positive early endosomes (Guiducci et al., 2006; Honda et al., 2005). Although enhanced ODN uptake and, consequently, increased endosomal ligand concentrations are clearly responsible for the TLR9-dependent cytokine induction by PD non-CpG ODNs in myeloid DCs, poly-G- or DOTAP-mediated complex formation both have an additional effect that allows induction of α-interferon production in plasmacytoid DCs, i.e., temporal retention of ODN ligands in early endosomal compartments. Complexed PD non-CpG ODNs thus induce IFN-α production in pDCs because of increased ligand concentrations in early endosomes. Importantly, none of the above mentioned stimulatory effects were seen in *Tlr9*$^{-/-}$ cells, suggesting that cytosolic DNA sensors do not participate in ODN recognition. We conclude that not only CpG ODNs but also PD non-CpG ODNs can trigger robust TLR9 activation in both pDCs and cDCs upon enforced endosomal translocation. Our data thus help to explain why natural "self-DNA" poor in unmethylated CpG motifs can drive TLR9 activation.

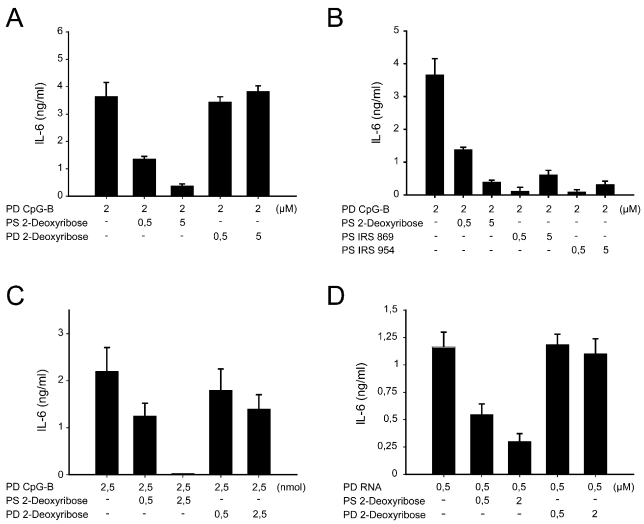

Figure 6. PS 2′ Deoxyribose Homopolymer Is a TLR9 and TLR7 Antagonist

(A) WT Flt3L-DCs (1 × 10^6/well) were incubated for 18 hr with 2 μM stimulatory PD CpG-B ODN ± indicated concentrations of PS or PD 2′ deoxyribose backbone molecules. IL-6 concentrations were detected in culture supernatants by enzyme-linked immunosorbant assay.

(B) WT Flt3L-DCs (1 × 10^6/well) were incubated for 18 hr with 2 μM stimulatory PD CpG-B ODN ± indicated concentrations of PS 2′ deoxyribose (20-mer) or PS IRS ODNs. IL-6 concentrations were detected in culture supernatants by enzyme-linked immunosorbant assay. Portions of this graph are from the same set of experiments as in (A).

(C) C57BL6 WT mice were injected i.v. with 2.5 nmol PD CpG-B ODNs ± indicated amounts of PS or PD 2′ deoxyribose (20-mer), all complexed to DOTAP. Blood samples were obtained 2 hr after injection. Serum IL-6 concentrations were detected by enzyme-linked immunosorbant assay.

(D) WT Flt3L-DCs (1 × 10^6/well) were incubated for 18 hr with 0.5 μM of TLR7-stimulatory PD RNA (ORN AP-1) complexed to DOTAP. Indicated concentrations of PS or PD 2′ deoxyribose (20-mer) had been added to the culture 15 min prior to stimulation. IL-6 concentrations were detected in culture supernatants by enzyme-linked immunosorbant assay. Mean values and standard deviations of three independent experiments are shown in (A)–(D).

PS-based IRS ODN 865 and 661 have been reported to block TLR9 or TLR7 activation in a sequence-dependent manner, respectively (Barrat et al., 2005). Analyzing ligand affinities of TLR9 and TLR7 with a recently described luminescent-proximity assay (AlpaScreen [Latz et al., 2007]), we demonstrated high-affine binding of PS 2′ deoxyribose (20-mer) to TLR9 and TLR7 but did not detect agonist function. Instead, base-free PS 2′ deoxyribose efficiently inhibited ligand-driven TLR9 and TLR7 activation, as did PS-modified ODN lacking CpG motifs. These findings suggest that the PS 2′ deoxyribose backbone within PS-modified ODNs lacking CpG motifs is an important mediator of TLR9 and TLR7 antagonism. Obviously, in IRS ODNs, certain DNA bases bias the inhibitory effect of PS 2′ deoxyribose either toward TLR9 or TLR7 inhibition. In fact, similar to PS IRS ODNs, PS 2′ deoxyribose homopolymers may manifest therapeutic potential as immunopharmacons for ablation of TLR9 and/or TLR7 activation in certain autoimmune diseases such as lupus erythematosus (Barrat et al., 2005) or psoriasis (Lande et al., 2007). Analysis of animal models that mimic human autoimmune diseases will help to answer this question.

Compared to TLR9, ligand interaction and activation of TLR7 appear to follow different rules. Although we found ribose-backbone-instructed TLR7 activation through base-bearing, non-uracil ribose molecules (ribose-AP-1; ribose 1668), no inherent

stimulatory activity of base-free PD or PS ribose polymers was detected, despite specific binding of the base-free ribose backbone to TLR7. In contrast to TLR9, shown here to be 2′ deoxyribose sugar backbone-specific, TLR7 activation does not strictly depend on a ribose backbone because poly-U-2′ deoxyribose stimulated TLR7 (our data and Diebold et al., 2006). Moreover, PS 2′ deoxyribose efficiently inhibited ligand-induced TLR7 activation in vitro, as do TLR7-inhibiting PS IRS ODNs (Barrat et al., 2005). These data complement the striking ability of TLR7 to bind not only base-free ribose sugar backbones or ORNs but also 2′ deoxyribose sugar backbones or ODNs, with affinities very similar to TLR9. Hence, nucleic-acid recognition by TLR7 is not completely RNA sugar backbone specific.

In search of a mechanistic explanation for 2′ deoxyribose specificity of TLR9, we performed sequence and structure alignments with dsRNA-specific hTLR3, the only nucleotide-specific TLR with a crystal structure available to date (Choe et al., 2005). Overall, 27% of all amino acids (aa) are conserved between hTLR3 and hTLR9, and protein domains are roughly overlapping. The only hTLR3-ect residue that has been directly linked to recognition of ribose-specific 2′ OH groups is asparagine N541 (Bell et al., 2006), which, in hTLR9, corresponds to arginine (R639). mTLR9, instead of R639, possesses an R residue in close proximity (R645). We propose that R is well suited to differentially mediate 2′ H but not 2′ OH binding, first because of steric constraints, with the R side chain occupying more space than N, thus favoring 2′ H instead of 2′ OH entry into the binding site. Second, R commonly binds phosphate anions because of its positively charged guanidino group and is therefore often found in the active binding site of phosphorylated substrate binders. For firm conclusions, however, analysis of crystal structures of TLR9 binding either natural PD or PS-modified nucleic acids will be essential.

Dimerization is a common theme in models of TLR activation (Kindrachuk et al., 2007; Latz et al., 2007; Weber et al., 2003). Induction of TLR9 activity has been shown to involve ligand-induced conformational changes in constitutive TLR9 homodimers, causing close approximation of cytoplasmic TIR domains (Latz et al., 2007). On the basis of our data, we propose that the low-affine PD DNA sugar backbone drives such conformational changes in TLR9 homodimers, whereas separate recognition of nucleic acids provides enhanced ligand-receptor affinity and activation, possibly through a mechanism involving intramolecular or intermolecular positive cooperativity. Perhaps because of steric hindrance from the large sulfur atom, which also creates a new chiral center, inhibitory PS 2′ deoxyribose, despite high TLR9 affinity, cannot induce such basic conformational changes in preformed TLR9 dimers, unless aided by CpG motifs.

The DNA-methylation pattern differs between mammalian and prokaryotic genes. It is believed that CpG motifs, mainly modified by methylation in the mammalian genome but abundant in their unmethylated form in prokaryotic organisms, represent a critical determinant for the mammalian immune system to discriminate foreign invaders or pathogens from "self." In accordance with this concept, only unmethylated CpG motifs are thought to drive TLR9 activation and thus act as PAMPs. Our data challenge this view. We show that CpG-motif dependency exclusively characterizes PS-modified ODNs, whereas PD ODNs short of CpG motifs activate TLR9. Mechanistically, these properties of natural PD ODNs versus PS-modified ODNs are determined by the DNA sugar backbone 2′ deoxyribose, which per se acts as a TLR9 agonist (PD) or TLR9 antagonist (PS). It therefore seems reasonable to propose that evolutionary pressure has exiled DNA-recognizing TLR9 from the cell surface to intracellular compartments to avoid activation by extracellular host-derived DNA. Confined to endosomes, TLR9 is perfectly positioned to alert the host to DNA from invading pathogens, whereas "self-DNA" recognition occurs only upon enforced endosomal translocation.

EXPERIMENTAL PROCEDURES

Reagents

CpG-A ODNs (2216) was from Coley Pharmaceuticals. Other ODNs were commercially synthesized by TIB Molbiol. PD and PS 2′ deoxyribose 20-mer was synthesized by IBA GmbH and TIB Molbiol. PD/PS ribose 20-mer (±5′-FAM/carboxyfluorescein succinimidyl ester; ±3′-Biotin according to experimental requirements), ORN AP-1, DNA/RNA hybrid molecules, and ODNs 5′ labeled with Cy3 or Cy5 were from IBA GmbH. 2′ deoxyribose 5-phosphate monomer was from Sigma-Aldrich.

Antibodies

α-mouse B220-PE and α-mouse CD86-PE antibodies were from BD Biosciences. α-mouse 120G8 (-FITC or -Biotin) antibody (Asselin-Paturel et al., 2003) was provided by A. Krug.

Mice

All mice were on C57BL6 genetic background. Male WT mice (Jackson), male *Tlr9*$^{-/-}$, *Tlr7*$^{-/-}$ and *Tlr7*$^{-/-}$ *Tlr9*$^{-/-}$ mice (provided by S. Akira) and male *Irf7*$^{-/-}$ mice (provided by T. Taniguchi) were bred at our SPF animal facility according to German federal regulations and institutional guidelines.

Preparation of DC

Bone-marrow cells were harvested from mouse femurs and tibias and cultured for 8 days in complete RPMI (RPMI 1640 with L-glutamine, heat-inactivated 10% FCS, 100 μg/ml streptomycin, and 50 μM 2′ mercaptoethanol; all from PAA Laboratories) conditioned with recombinant murine Flt3-ligand (WEHI).

Cell Sorting

Flt3L-DC subsets were highly enriched by FACS sorting (FACS Aria, BD Biosciences) after staining with α-120G8-FITC (Asselin-Paturel et al., 2003) and α-B220-PE antibodies. Discrimination between live and dead cells was performed with propidium iodide (Invitrogen). The purity of the sorted cells was controlled on a CyAn ADP Lx (Dako) and found to be >99%.

Cell Stimulation

Flt3L-DCs were suspended in 500 μl RPMI 1640 with 10% FCS and 50 μM 2′ mercaptoethanol (all from PAA Laboratories) on 24-well plates and incubated for indicated times at indicated concentrations with ODNs, hybrids, backbone molecules, or controls. For measurement of cytokine induction, culture supernatants were collected for analysis by enzyme-linked immunosorbant assay (ELISA) specific for mouse IL-6 (BD Biosciences) and mouse IFN-α (compiled from rat anti-mouse interferon-α antibody [Tebu-Bio], rabbit anti-mouse interferon-α antibody [Tebu-Bio], POX-donkey anti-rabbit IgG antibody [Jackson]). For analysis of surface markers, cells were harvested, washed 2× with ice-cold PBS/3% FCS, incubated with α-CD86 PE antibody for 0.5 hr, washed 2×, fixed with 2% paraformaldehyde, and analyzed by fluorescence-activated cell sorting (FACS).

For complex formation with DOTAP (Roche), ODNs, hybrids, backbone molecules, and controls were suspended in 50 μl Opti-Mem (Invitrogen), combined with 50 μl DOTAP solution (10 μg in Opti-Mem), incubated for 15 min at room temperature, and added to cells.

ODN Uptake

ODN uptake was measured as described (Roberts et al., 2005). In brief, 0.5 × 10^6 Flt3L-DC were incubated with Cy5-labeled ODNs for 45 min in 500 μl complete RPMI. Harvested cells were washed with ice-cold PBS, incubated with 12.5 mg/ml dextran sulfate (Sigma) for 10 min on ice (for removal of ODN bound to the cell surface), washed in PBS, fixed with 2% paraformaldehyde, and analyzed by fluorescence-activated cell sorting (FACS).

I.V. Injection and Collection of Blood Samples

C57BL6 WT mice were injected with preprepared DOTAP complexes (30 μl DOTAP at final volume of 200 μl in sterile PBS) of 2.5 nmol stimulatory PD CpG-B-ODN 1668 alone or in combination with 0.5 nmol or 2.5 nmol 2′ deoxyribose backbone molecules (20-mers; PS or PD) into the tail vein. After 2 hr, mice were sacrificed and blood samples were collected by intracardial puncture. Samples were centrifuged after coagulation was complete. Serum was used for analysis by enzyme-linked immunosorbant assay.

Human TLR-Fc Protein Purification

hTLR9-Fc protein was purified from lysates of HEK293 cells stably expressing a fusion protein containing the ectodomain of human TLR9 linked to the Fc portion of mouse IgG2a. Cells were grown in serum-free media (CD293, Invitrogen), harvested by centrifugation, washed twice in ice-cold PBS, and lysed in lysis buffer on ice (1% CHAPS, 50 mM Tris-Cl, 150 mM NaCl, 1 mM EDTA, 10% glycerol, 12 mM 2′ mercaptoethanol, and complete protease inhibitors [Roche]). After pelleting nuclei at 14.000 × g and 0.45 μm filtration of the lysates (Sartobran 300, Sartorius), we captured the protein by protein A chromatography (Amersham) at 4°C with automated FPLC. After extensive washing of the columns in lysis buffer, the protein was eluted by a continuous gradient from pH 7.4 to pH 3 (low pH buffer: 50 mM citric acid [pH 3], 150 mM NaCl, 1 mM EDTA, 10% glycerol, and 12 mM 2′ mercaptoethanol). The low pH was neutralized by addition of one-tenth of the volume 1 M Tris-Cl, pH 8 into each of the fractions. As a polishing step, purified hTLR9-Fc was separated by size-exclusion chromatography (superose 6, Amersham), and hTLR9-Fc containing fractions were pooled and concentrated. hTLR7-Fc and hTLR2-Fc proteins were purified as above. Here, the cells stably expressed a fusion protein containing the ectodomain of hTLR7 or hTLR2, linked to the Fc portion of mouse IgG2a.

Murine TLR-Fc Protein Purification

mTLR9-Fc and mTLR2-Fc proteins were obtained and purified as described in (Rutz et al., 2004).

SPR Biosensor Analysis

ODN binding of mTLR9-ect or mTLR2-ect was analyzed in a Biacore X device (Biacore AB) on SA chips at 25°C. In brief, the biotinylated ODN were diluted to a final concentration of 100 nM in 50 mM MES, pH 6.5, supplemented with 150 mM NaCl and 1 mM $MgCl_2$ (which was also used as running buffer in all SPR biosensor measurements), and bound at equimolar immobilization levels (~1700 RU for PD CpG-B ODN 1668 and PD non-CpG ODN AP1, ~600 RU for C3-spacer, PD 2′ deoxyribose, and PD ribose homopolymers) to the SA in one of the two flow cells. The second flow cell served as a blank control for the subtraction of nonspecific analyte binding and of bulk refractive index background. For SPR monitoring of the mTLR9-ect or mTLR2-ect interaction to the surface immobilized ODNs, 45 μl of 100 nM recombinant protein in running buffer was injected into the biosensor at a flow rate of 10 μl/min. After a 300 s dissociation period, the biosensor chip was regenerated by two 5 μl injections of a solution containing 50 mM NaOH and 1 M NaCl and extensive re-equilibration in running buffer.

Competitive binding analyses were performed by 10 min pre-incubation of 200 nM mTLR9-ect with the PD or PS variants of 2′ deoxyribose (20-mer), non-CpG ODN AP-1 and IRS ODN 869 at concentrations of 0.01, 0.1, 1 and 10 mM and subsequent injection of the mixture over a PD CpG-B ODN 1668 coupled biosensor surface.

AlphaScreen TLR Binding Assay

The AlphaScreen (amplified luminescent-proximity homogeneous assay) was set up as an association assay. TLR-ect-Fc protein was incubated with biotinylated ligand in 50 mM HEPES, pH 6.5, 150 mM NaCl, 5 mM EDTA, 0.1% BSA, and 0.01% Tween 20 for 60 min. Subsequently, protein-A-coated acceptor beads and streptavidin-coated donor beads (Alphascreen beads, Perkin Elmer) were added from 5× stock concentrations. After 30 min incubation at 25°C in the dark, samples in white 384-well plates (Proxiplate, Perkin Elmer) were read with the Envision HT microplate reader (Perkin Elmer). Data were analyzed by GraphPad Prism version 4.00 for Macintosh (GraphPad Software).

SUPPLEMENTAL DATA

Five figures are available at http://www.immunity.com/cgi/content/full/28/3/315/DC1/.

ACKNOWLEDGMENTS

We thank H. Drexler for excellent technical assistance, M. Schiemann for FACS-sorting of DC subsets, A. Krug for providing α-mouse 120G8 antibodies, and T. Sparwasser and the Walter and Eliza Hall Institute of Medical Research (Australia) for providing the CHO cell line expressing FLAG-tagged murine Flt3-ligand. We further wish to thank S. Akira and T. Taniguchi who generously provided breeding pairs for the knockout mice used. Thanks to D. Busch, G. Häcker, and L. Layland for critically reading the manuscript. Special thanks to C. Cirl for help with protein analysis and modeling. This work was supported by Sonderforschungsbereich (SFB) 456 and the Nationales Genomforschungsnetz (NGFN) 2, all grants to H.W.

Received: October 29, 2007
Revised: December 17, 2007
Accepted: January 15, 2008
Published online: March 13, 2008

REFERENCES

Akira, S., Uematsu, S., and Takeuchi, O. (2006). Pathogen recognition and innate immunity. Cell *124*, 783–801.

Alexopoulou, L., Holt, A.C., Medzhitov, R., and Flavell, R.A. (2001). Recognition of double-stranded RNA and activation of NF-kappaB by Toll-like receptor 3. Nature *413*, 732–738.

Asselin-Paturel, C., Brizard, G., Pin, J.J., Briere, F., and Trinchieri, G. (2003). Mouse strain differences in plasmacytoid dendritic cell frequency and function revealed by a novel monoclonal antibody. J. Immunol. *171*, 6466–6477.

Barrat, F.J., Meeker, T., Gregorio, J., Chan, J.H., Uematsu, S., Akira, S., Chang, B., Duramad, O., and Coffman, R.L. (2005). Nucleic acids of mammalian origin can act as endogenous ligands for Toll-like receptors and may promote systemic lupus erythematosus. J. Exp. Med. *202*, 1131–1139.

Barton, G.M., Kagan, J.C., and Medzhitov, R. (2006). Intracellular localization of Toll-like receptor 9 prevents recognition of self DNA but facilitates access to viral DNA. Nat. Immunol. *7*, 49–56.

Bauer, S., Kirschning, C.J., Hacker, H., Redecke, V., Hausmann, S., Akira, S., Wagner, H., and Lipford, G.B. (2001). Human TLR9 confers responsiveness to bacterial DNA via species-specific CpG motif recognition. Proc. Natl. Acad. Sci. USA *98*, 9237–9242.

Bell, J.K., Askins, J., Hall, P.R., Davies, D.R., and Segal, D.M. (2006). The dsRNA binding site of human Toll-like receptor 3. Proc. Natl. Acad. Sci. USA *103*, 8792–8797.

Beutler, B., Jiang, Z., Georgel, P., Crozat, K., Croker, B., Rutschmann, S., Du, X., and Hoebe, K. (2006). Genetic analysis of host resistance: Toll-like receptor signaling and immunity at large. Annu. Rev. Immunol. *24*, 353–389.

Bird, A.P. (1986). CpG-rich islands and the function of DNA methylation. Nature *321*, 209–213.

Bishop, J.S., Guy-Caffey, J.K., Ojwang, J.O., Smith, S.R., Hogan, M.E., Cossum, P.A., Rando, R.F., and Chaudhary, N. (1996). Intramolecular G-quartet motifs confer nuclease resistance to a potent anti-HIV oligonucleotide. J. Biol. Chem. *271*, 5698–5703.

Boule, M.W., Broughton, C., Mackay, F., Akira, S., Marshak-Rothstein, A., and Rifkin, I.R. (2004). Toll-like receptor 9-dependent and -independent dendritic

cell activation by chromatin-immunoglobulin G complexes. J. Exp. Med. *199*, 1631–1640.

Choe, J., Kelker, M.S., and Wilson, I.A. (2005). Crystal structure of human toll-like receptor 3 (TLR3) ectodomain. Science *309*, 581–585.

Dalpke, A.H., Zimmermann, S., Albrecht, I., and Heeg, K. (2002). Phosphodiester CpG oligonucleotides as adjuvants: Polyguanosine runs enhance cellular uptake and improve immunostimulative activity of phosphodiester CpG oligonucleotides in vitro and in vivo. Immunology *106*, 102–112.

Diebold, S.S., Kaisho, T., Hemmi, H., Akira, S., and Reis e Sousa, C. (2004). Innate antiviral responses by means of TLR7-mediated recognition of single-stranded RNA. Science *303*, 1529–1531.

Diebold, S.S., Massacrier, C., Akira, S., Paturel, C., Morel, Y., and Reis e Sousa, C. (2006). Nucleic acid agonists for Toll-like receptor 7 are defined by the presence of uridine ribonucleotides. Eur. J. Immunol. *36*, 3256–3267.

Duramad, O., Fearon, K.L., Chang, B., Chan, J.H., Gregorio, J., Coffman, R.L., and Barrat, F.J. (2005). Inhibitors of TLR-9 act on multiple cell subsets in mouse and man in vitro and prevent death in vivo from systemic inflammation. J. Immunol. *174*, 5193–5200.

Guiducci, C., Ott, G., Chan, J.H., Damon, E., Calacsan, C., Matray, T., Lee, K.D., Coffman, R.L., and Barrat, F.J. (2006). Properties regulating the nature of the plasmacytoid dendritic cell response to Toll-like receptor 9 activation. J. Exp. Med. *203*, 1999–2008.

Gursel, I., Gursel, M., Yamada, H., Ishii, K.J., Takeshita, F., and Klinman, D.M. (2003). Repetitive elements in mammalian telomeres suppress bacterial DNA-induced immune activation. J. Immunol. *171*, 1393–1400.

Hacker, H., Mischak, H., Miethke, T., Liptay, S., Schmid, R., Sparwasser, T., Heeg, K., Lipford, G.B., and Wagner, H. (1998). CpG-DNA-specific activation of antigen-presenting cells requires stress kinase activity and is preceded by non-specific endocytosis and endosomal maturation. EMBO J. *17*, 6230–6240.

Heil, F., Hemmi, H., Hochrein, H., Ampenberger, F., Kirschning, C., Akira, S., Lipford, G., Wagner, H., and Bauer, S. (2004). Species-specific recognition of single-stranded RNA via toll-like receptor 7 and 8. Science *303*, 1526–1529.

Hemmi, H., Takeuchi, O., Kawai, T., Kaisho, T., Sato, S., Sanjo, H., Matsumoto, M., Hoshino, K., Wagner, H., Takeda, K., and Akira, S. (2000). A Toll-like receptor recognizes bacterial DNA. Nature *408*, 740–745.

Honda, K., Ohba, Y., Yanai, H., Negishi, H., Mizutani, T., Takaoka, A., Taya, C., and Taniguchi, T. (2005). Spatiotemporal regulation of MyD88-IRF-7 signalling for robust type-I interferon induction. Nature *434*, 1035–1040.

Janeway, C.A., Jr., and Medzhitov, R. (2002). Innate immune recognition. Annu. Rev. Immunol. *20*, 197–216.

Kerkmann, M., Costa, L.T., Richter, C., Rothenfusser, S., Battiany, J., Hornung, V., Johnson, J., Englert, S., Ketterer, T., Heckl, W., et al. (2005). Spontaneous formation of nucleic acid-based nanoparticles is responsible for high interferon-alpha induction by CpG-A in plasmacytoid dendritic cells. J. Biol. Chem. *280*, 8086–8093.

Kindrachuk, J., Potter, J.E., Brownlie, R., Ficzycz, A.D., Griebel, P.J., Mookherjee, N., Mutwiri, G.K., Babiuk, L.A., and Napper, S. (2007). Nucleic acids exert a sequence-independent cooperative effect on sequence-dependent activation of Toll-like receptor 9. J. Biol. Chem. *282*, 13944–13953.

Krieg, A.M. (2002). CpG motifs in bacterial DNA and their immune effects. Annu. Rev. Immunol. *20*, 709–760.

Lande, R., Gregorio, J., Facchinetti, V., Chatterjee, B., Wang, Y.H., Homey, B., Cao, W., Wang, Y.H., Su, B., Nestle, F.O., et al. (2007). Plasmacytoid dendritic cells sense self-DNA coupled with antimicrobial peptide. Nature *449*, 564–569.

Latz, E., Schoenemeyer, A., Visintin, A., Fitzgerald, K.A., Monks, B.G., Knetter, C.F., Lien, E., Nilsen, N.J., Espevik, T., and Golenbock, D.T. (2004). TLR9 signals after translocating from the ER to CpG DNA in the lysosome. Nat. Immunol. *5*, 190–198.

Latz, E., Verma, A., Visintin, A., Gong, M., Sirois, C.M., Klein, D.C., Monks, B.G., McKnight, C.J., Lamphier, M.S., Duprex, W.P., et al. (2007). Ligand-induced conformational changes allosterically activate Toll-like receptor 9. Nat. Immunol. *8*, 772–779.

Leadbetter, E.A., Rifkin, I.R., Hohlbaum, A.M., Beaudette, B.C., Shlomchik, M.J., and Marshak-Rothstein, A. (2002). Chromatin-IgG complexes activate B cells by dual engagement of IgM and Toll-like receptors. Nature *416*, 603–607.

Leifer, C.A., Brooks, J.C., Hoelzer, K., Lopez, J., Kennedy, M.N., Mazzoni, A., and Segal, D.M. (2006). Cytoplasmic targeting motifs control localization of toll-like receptor 9. J. Biol. Chem. *281*, 35585–35592.

Leifer, C.A., Kennedy, M.N., Mazzoni, A., Lee, C., Kruhlak, M.J., and Segal, D.M. (2004). TLR9 is localized in the endoplasmic reticulum prior to stimulation. J. Immunol. *173*, 1179–1183.

Roberts, T.L., Dunn, J.A., Terry, T.D., Jennings, M.P., Hume, D.A., Sweet, M.J., and Stacey, K.J. (2005). Differences in macrophage activation by bacterial DNA and CpG-containing oligonucleotides. J. Immunol. *175*, 3569–3576.

Rutz, M., Metzger, J., Gellert, T., Luppa, P., Lipford, G.B., Wagner, H., and Bauer, S. (2004). Toll-like receptor 9 binds single-stranded CpG-DNA in a sequence- and pH-dependent manner. Eur. J. Immunol. *34*, 2541–2550.

Sester, D.P., Naik, S., Beasley, S.J., Hume, D.A., and Stacey, K.J. (2000). Phosphorothioate backbone modification modulates macrophage activation by CpG DNA. J. Immunol. *165*, 4165–4173.

Verthelyi, D., Ishii, K.J., Gursel, M., Takeshita, F., and Klinman, D.M. (2001). Human peripheral blood cells differentially recognize and respond to two distinct CPG motifs. J. Immunol. *166*, 2372–2377.

Weber, A.N., Tauszig-Delamasure, S., Hoffmann, J.A., Lelievre, E., Gascan, H., Ray, K.P., Morse, M.A., Imler, J.L., and Gay, N.J. (2003). Binding of the *Drosophila* cytokine Spatzle to Toll is direct and establishes signaling. Nat. Immunol. *4*, 794–800.

Yasuda, K., Rutz, M., Schlatter, B., Metzger, J., Luppa, P.B., Schmitz, F., Haas, T., Heit, A., Bauer, S., and Wagner, H. (2006). CpG motif-independent activation of TLR9 upon endosomal translocation of "natural" phosphodiester DNA. Eur. J. Immunol. *36*, 431–436.

Yasuda, K., Yu, P., Kirschning, C.J., Schlatter, B., Schmitz, F., Heit, A., Bauer, S., Hochrein, H., and Wagner, H. (2005). Endosomal translocation of vertebrate DNA activates dendritic cells via TLR9-dependent and -independent pathways. J. Immunol. *174*, 6129–6136.